[CANCER RESEARCH 61, 131–137, January 1, 2001]

Characterization of the Antitumor Effects of the Selective Farnesyl Protein Transferase Inhibitor R115777 *in Vivo* and *in Vitro*

David W. End,[1] Gerda Smets, Alison V. Todd, Tanya L. Applegate, Caroline J. Fuery, Patrick Angibaud, Marc Venet, Gerard Sanz, Herve Poignet, Stacy Skrzat, Ann Devine, Walter Wouters, and Charles Bowden

Department of Medicinal Chemistry, Janssen Research Foundation, Val De Reuil 27106, France [M. V., H. P., P. A., G. S.]; Department of Oncology, Janssen Research Foundation, Beerse B2340, Belgium [G. S., W. W.]; Johnson and Johnson Research Pty., Ltd., Strawberry Hills, New South Wales 2011, Australia [A. V. T., T. L. A., C. J. F.]; and Department of Oncology, Janssen Research Foundation, Spring House, Pennsylvania 19477 [D. W. E., S. S., A. D., C. B.]

ABSTRACT

R115777 {(B)-6-[amino(4-chlorophenyl)(1-methyl-*1H*-imidazol-5-yl)-methyl]-4-(3-chlorophenyl)-1-methyl-*2(1H)*-quinolinone} is a potent and selective inhibitor of farnesyl protein transferase with significant antitumor effects *in vivo* subsequent to oral administration in mice. *In vitro*, using isolated human farnesyl protein transferase, R115777 competitively inhibited the farnesylation of lamin B and K-RasB peptide substrates, with IC_{50}s of 0.86 nM and 7.9 nM, respectively. In a panel of 53 human tumor cell lines tested for growth inhibition, ~75% were found to be sensitive to R115777. The majority of sensitive cell lines had a wild-type *ras* gene. Tumor cell lines bearing H-*ras* or N-*ras* mutations were among the most sensitive of the cell lines tested, with responses observed at nanomolar concentrations of R115777. Tumor cell lines bearing mutant K-*ras* genes required higher concentrations for inhibition of cell growth, with 50% of the cell lines resistant to R115777 up to concentrations of 500 nM. Inhibition of H-Ras, N-Ras, and lamin B protein processing was observed at concentrations of R115777 that inhibited cell proliferation. However, inhibition of K-RasB protein-processing could not be detected. Oral administration b.i.d. of R115777 to nude mice bearing s.c. tumors at doses ranging from 6.25–100 mg/kg inhibited the growth of tumors bearing mutant H-*ras*, mutant K-*ras*, and wild-type *ras* genes. Histological evaluations revealed heterogeneity in tumor responses to R115777. In LoVo human colon tumors, treatment with R115777 produced a prominent antiangiogenic response. In CAPAN-2 human pancreatic tumors, an antiproliferative response predominated, whereas in C32 human melanoma, marked induction of apoptosis was observed. The heterogeneity of histological changes associated with antitumor effects suggested that R115777, and possibly farnesyl protein transferase inhibitors as a class, alter processes of transformation related to tumor-host interactions in addition to inhibiting tumor-cell proliferation.

INTRODUCTION

The Ras proteins have been the focus of oncology drug discovery efforts because of some unique features of the cellular metabolism of these proteins. To function in signal transduction and cell transformation, Ras must attach to the plasma membrane. This membrane localization is required for interactions with membrane receptors and the SH2/SH3 domain adaptor proteins Grb2 and SOS as well as for activation of a downstream effector(s) such as Raf protein kinase (1–4). Newly synthesized Ras proteins must be posttranslationally modified in mammalian cells by farnesylation and then by the proteolytic cleavage of the three terminal amino acids and carboxy-*O*-methylation to produce the hydrophobicity or recognition sites that allow proper membrane localization (5–7). The initial step catalyzed by FPT[2] involves the covalent attachment of farnesol via a thioether linkage to a cysteine residue positioned four amino acids from the COOH-terminus of the protein (5, 8). The enzyme requires only the four COOH-terminal amino acids or CAAX motif for specific binding and catalysis of protein substrates.

The characterization of FPT and tetrapeptide inhibitors of the enzyme set off a search for low-molecular weight, nonpeptide inhibitors that could be developed as therapy-selective for tumors bearing *ras* mutations (9). Initial studies with peptidomimetic compounds suggested that FTIs could, in fact, selectively inhibit the growth of *ras*-transformed cells (10–12). However, as experience with FTIs increased, the role of ras proteins in mediating the antitumor effects of this class of agent became less certain (13). As has been reported previously and in the current studies, FTIs have shown antiproliferative activity in tumor cell lines devoid of *ras* mutations (14). Also, the different H-Ras, N-Ras, and K-RasB isoforms were found to behave quite differently in the presence of FTIs. With isolated enzyme, the K-RasB protein demonstrated a higher affinity for FPT, which decreased the potency of FTIs competitive for the CAAX binding site (15). In intact tumor cells, the mutant, activated K-RasB and N-ras isoforms were associated with resistance to FTIs attributable to alternative processing by the parallel pathway of geranylgeranylation via GGPT I (16–18). However, as will be described, R115777 and other inhibitors have shown antiproliferative and antitumor activity in tumor cell lines bearing K-*ras* mutations (19, 20). At the moment, there is discordance between the antitumor activity of FTIs and the biology of Ras proteins. Several molecular targets such as RhoB and centromere-associated proteins (21–24) have emerged as possible downstream effectors for the FTIs. Treatment of cells with the FTI L-739,749 induced an alternative processing of RhoB via PGGT I, with a gain of geranylgeranylated RhoB and concomitant reduction of the farnesylated RhoB (21). The accumulation of geranylgeranylated RhoB was associated with antiproliferative effects. Also in support of these observations, transfection of RhoB with CAAX motifs that restrict prenylation to geranylgeranylation reproduced many of the effects of FTI treatment, including reversal of the transformed phenotype as well as induction of apoptosis (23). However, recent studies have shown that expression of either farnesylated RhoB or geranygeranylated RhoB produced similar tumor suppressive activity (25). Thus, the role of RhoB in the effects of FTIs is uncertain. Additionally, inhibition of the farnesylation of the centromere-associated proteins CENP-E and CENP-F has been linked to a G_2-M growth arrest observed in some tumor cells *in vitro* (24). The current evidence suggests a role for multiple prenylated effectors in mediating the antitumor effects of FTIs. Involvement of multiple effectors might also be manifested as heterogeneous responses at the level of the tumor cell or intact tumors.

The current studies describe the preclinical pharmacology of R115777, a novel imidazole FTI that has entered Phase III clinical

Received 5/23/00; accepted 11/1/00.

The costs of publication of this article were defrayed in part by the payment of page charges. This article must therefore be hereby marked *advertisement* in accordance with 18 U.S.C. Section 1734 solely to indicate this fact.

[1] To whom requests for reprints should be addressed, at Department of Oncology, Janssen Research Foundation, Spring House, PA 19477. Phone: (215) 628-5974; Fax: (215) 628-5047; E-mail: dend@prius.jnj.com.

[2] The abbreviations used are: FPT, farnesyl protein transferase; FTI, farnesyl protein transferase inhibitor; GGPT I, geranygeranyl protein transferase type I; R115777, (B)-6-[amino(4-chlorophenyl)(1-methyl-*1H*-imidazol-5-yl)methyl]-4-(3chlorophenyl)-1-methyl-*2(1H)*-quinolinone; ISEL, *in situ* end labeling; VEGF, vascular endothelial cell growth factor; b.i.d., twice daily.

trials. Our findings will be discussed in relationship to the *ras* status of tumor cell lines as well as the heterogeneity of tissue responses observed in three human tumor xenografts after *in vivo* treatment with R115777.

MATERIALS AND METHODS

Compound. R115777 was synthesized as a racemate and purified as a single enantiomer by high-performance liquid chromatography.[3] The structure is presented in Fig. 1.

Materials. Human tumor cell lines were purchased from the American Type Culture Collection (Rockville, MD). NIH 3T3 cells transfected with the activated T24 H-*ras* oncogene (T24 cells) or with activated Raf were obtained from Dr. Richard Connors, Janssen Research Foundation (Spring House, PA). The Farnesyl Protein Transferase Scintillation Proximity Assay, including the lamin B peptide substrate and the radiolabeled [^{3}H]-farnesyl PP_I, was purchased from Amersham Life Sciences (Arlington, Heights, IL). The PGGT I peptide substrate biotinYRASNRSCAIL was synthesized at Multiple Peptide Systems (San Diego, CA). [^{3}H]-geranylgeranylpyrophosphate was from DuPont NEN (Billerica, MA). The K-RasB peptide substrate biotin-KKKKKKSKTKCVIM was synthesized at the Robert Wood Johnson Pharmaceutical Research Institute Johnson and Johnson Biotechnology Center (La Jolla, CA). Antibodies to the Ras protein, v-H-Ras (Ab-1) conjugated to agarose, pan-Ras Ab-3, and RhoB were purchased from Oncogene Research Products (Cambridge, MA). Antibody to Rap 1A/krev was from Santa Cruz Biotechnology (Santa Cruz, CA). The secondary antibody anti-mouse IgG conjugated to horseradish peroxidase and the Enhanced Chemiluminescence reagents were purchased from Amersham Life Sciences. Precast 10–20% SDS polyacrylamide slab gels were obtained from Integrated Separation Systems (Natick, MA). The primary antibodies used for immunocytochemistry included anti-BrdUrd clone BU-1 (Amersham, Buckinghamshire, United Kingdom), anti-Ki-67 clone MIB-1 (Novocastra, Newcastle upon Tyne, United Kingdom), anti-Factor VIII code A0082 (monoclonal; Dako, Glostrup, Denmark), and anti-VEGF A20 (Santa Cruz Biotechnology, Santa Cruz, CA).

Animals. Female nu/nu immunodeficient nude mice (42 days old) were purchased from Charles River Laboratories (Wilmington, MA). Mice were housed five per cage in microisolator cages placed in laminar flow shelving to maintain sterility. All bedding, food, water, and cages were autoclaved. Animals were handled within the sterile confines of a laminar flow cabinet. The mice were otherwise maintained under standard vivarium conditions. Tumor studies were conducted under a protocol approved by the Institutional Animal Care and Use Committee.

Isolation of FPT and PGGT 1. FPT and PGGT I were isolated from Kirsten virus-transformed human osteosarcoma cell tumors essentially as described by Reiss *et al.* (8, 26). Tumors were excised and immediately homogenized in buffer (3.0 ml/tumor) containing 50 mM Tris, 1 mM EDTA, 1 mM EGTA, and 0.2 mM phenylmethylsulfonylfluoride (pH 7.5). The homogenate was centrifuged 100,000 $\times$ *g* for 60 mi, and a 30–50% ammonium sulfate precipitate was prepared from the supernatant. After dialysis, FPT and PGGT 1 activity were further isolated by ion exchange chromatography on Fast Q Sepharose. FPT was measured using the Amersham Scintillation Proximity Assay using the lamin B peptide substrate (Biotin-YRASNRSCAIM) provided with the assay. In some studies, the K-rasB peptide (0.25 μM) was substituted for the lamin B peptide. PGGT 1 assays were performed using a modification of the Amersham Scintillation Proximity Assay methods. A biotin-YRASNRSCAIL peptide substrate was incubated with [1-[^{3}H](n)]geranylgeranylpyrophosphate for 120 min at 37°C. After terminating reactions, samples were equilibrated overnight before counting.

Cell Proliferation Assays. Trypsinized cell suspensions were inoculated into six-well cluster dishes at an initial density of 200,000 cells/well in 3 ml of complete growth medium. R115777 was added at concentrations ranging from 0.5–500 nM in 3 μl of DMSO. Cells were allowed to proliferate to high saturation densities beyond confluence for 4–7 days. Cell numbers were quantified by detaching cell monolayers in 1 ml of trypsin and counting cell suspensions on a Coulter particle counter.

[3] D. W. End, M. G. Venet, P. R. Angiband, and G. C. Sanz, the synthesis will be published elsewhere and can be found in patent WO 9716443 A1.

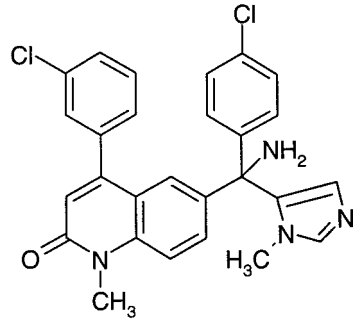

Fig. 1. Structure of R115777.

Analysis of Activating Mutations in *ras* Genes. DNA was prepared from human tumor cell monolayers using the DNAzol Reagent (Life Technologies, Inc.). An RFLP-PCR strategy was used to screen for activating mutations within K-*ras*, N-*ras* and H-*ras* (27). Exons 1 and 2 of all three *ras* genes were simultaneously amplified in a single multiplex reaction and an aliquot was used for a second round of PCR. Resistance to cleavage at natural or primer-induced restriction enzyme sites in second-round amplicons indicated the presence of a mutation that had abolished the site at the loci being analyzed. Restriction enzymes for the analysis of specific loci were *Bst*N I (K-*ras* codon 12), *Bsl* I (K-*ras* codon 13, N-*ras* codons 12 and 13), *Msc* I (H-*ras* codon 61; N-*ras* codon 61, positions 1 and 2), *Hae*III (K-*ras* codon 61, position 1), *Bfa* I (N-*ras* codon 61, position 3), and *Tru*9 I (K-*ras* codon 61, positions 2 and 3; H-*ras* intron D, position 2719). Reactions were digested overnight and PCR products were analyzed by gel electrophoresis. The correlation of *ras* mutation status *versus* sensitivity to R115777 were analyzed by a χ^2 test with sensitivity defined as 50% inhibition of cell proliferation at concentrations of $\leq$100 nM.

Analysis of Ras Protein Processing in Intact Cells in Culture. T24F1 or CAPAN-2 cells were grown as monolayers in T75 tissue culture flasks in 25 ml of complete growth medium. The monolayer cultures were treated with R115777 for 72 h. Then the growth medium was removed and the monolayers were washed once with 5 ml of PBS. Cells were harvested by scraping into ice-cold PBS and collected by centrifugation (100 $\times$ *g* for 5 min). Total cellular Ras processing was analyzed in particulate and soluble fractions of cells as described by Yan *et al.* (28). Detection of K-Ras immunoreactivity required immunoprecipitation with v-H-Ras antibody conjugated to agarose before electrophoresis and immunoblotting procedures. Protein determinations were performed on 5- to 10-μl samples of pellets and supernatants (29). Samples were normalized such that equal amounts of protein were added to Laemmli sample buffer and separated on 10–20% gradient SDS polyacrylamide slab gels. After transfer to polyvinylidene difluoride membranes, samples were incubated overnight at 4°C with primary antibodies. The immunostained antigens were visualized using horseradish peroxidase-conjugated secondary antibodies and Amersham enhanced chemiluminescence detection reagents.

Tumor Studies in Nude Mice. Tumor cell lines maintained as monolayer cultures were detached by trypsinization. Tumor cell suspensions were pooled and trypsin was inactivated by the addition of serum-containing medium. Cells were collected by centrifugation and washed once in HBSS. Cell suspensions were adjusted to a final concentration of 1×10^6 cells/0.1 ml of HBSS. Mice were inoculated with a single s.c. injection of 0.10 ml of tumor cell suspension in the inguinal region of the thigh. Mice were housed five per cage, with 15 mice randomly assigned to treatment groups. Three days after tumor inoculation, treatment with R115777 was initiated. R115777 was administered b.i.d. by oral gavage in a 20% β-cyclodextrin vehicle as a volume of 0.10 ml of solution/10 g body weight. Control groups received the same dosage/volume of the 20% β-cyclodextrin vehicle. Body weight and tumor size as determined by caliper measurements were monitored weekly. At the end of study, mice were sacrificed by CO_2 asphyxiation. Tumors were excised, weighed, and fixed immediately in 4% paraformaldehyde. ANOVA, mean values for treatment groups, and SE for *in vivo* parameters were calculated using IMSL subroutines compiled by R. W. Johnson of the Pharmaceutical Research Institute, Science Information Department, on a VAX computer. A value of $P < 0.05$ was considered significant.

Preparation of Tumors for Histology. Fixed tumors were cut into thin fragments (approximately 10 × 10 × 3 mm). The tissues were rinsed overnight in 0.1 M phosphate buffer (pH 7.4). After dehydration in acetone, LoVo and CAPAN-2 tumors were infiltrated and embedded in Technovit 8100 (Kulzer, Wehrheim, Germany). C32 melanoma tumors were dehydrated in ethanol/xylol and infiltrated in paraffin block. For Technovit embedding, infiltration and embedding were performed under a nitrogen atmosphere at 0°C. Sections (3 μm) were cut with a Leica Jung Autocut and mounted onto glass slides by drying at 50°C for 2 days. Paraffin sections were mounted with Biobound-coating (British Biocell International, Cardiff, United Kingdom). After staining with erythrosine B and hematoxylin, the slides were mounted with Pertex (LED Techno, Hechtel, Belgium).

Immunocytochemistry. Sections were treated with a 1:10 dilution of Target Unmasking Fluid (Sanbio, Uden, the Netherlands) by heating to 90°C in a microwave oven. Slides were incubated with 0.5% trypsin solutions for 30 min at 37°C. The slides were extensively rinsed, and then endogenous peroxidase was blocked by incubating with 1% peroxide in methanol for 15 min. Nonspecific antibody-binding sites were blocked by incubation with 0.5% lysozyme for 60 min. Incubations with the primary antibody were performed at room temperature at various times optimized for each antibody. Staining with the primary antibody was visualized using the biotin-avidin peroxidase method (Dako, Glostrup, Denmark) using Sigma Fast DAB (Sigma, St. Louis, MO) At the end of the procedure, the slides were counterstained with 0.25% methyl green. To monitor apoptosis, ISEL was performed according to the directions of the TACSTM1 Klenow Kit (Trevigen, Gaithersburg, MD).

Quantitative image analysis was performed using a Zeiss Axioplan microscope fitted with CCD cameras interfaced to a Silicon Graphics Indy R5000 Unix-based workstation. Image analysis routines were written in C under the SCIL-Image software package (SCIL Image, Version 1.3; TNO-TPD, Delft, the Netherlands). For evaluation of BrdUrd-labeling and apoptosis, images were taken with a black and white CCD camera (MX5, Adimec, the Netherlands). For quantification of cell proliferation, the total number of cells was obtained by imaging the methyl green staining through a 650-nm broadband interference filter. To obtain images of the nuclei labeled with BrdUrd, the same microscopic fields were viewed with a 450-nm broadband interference filter. For quantifying Factor VIII and VEGF-staining, 24-bit RGB color images were acquired with a cooled CCD-camera (Sony DXC-930 P) and transformed to HSI-space. The immunocytochemical signal was quantified as a percentage of the area in a field. For measurements of BrdUrd incorporation and apoptosis, a ×20 objective was used; whereas, for VEGF- and Factor VIII-staining, a ×40 objective was used. The total areas on each slide evaluated for BrdUrd incorporation and Ki-67 staining was 4 mm^2. Apoptosis was evaluated in an 8-mm^2 area. The total number of cells quantified ranged from 8,000–25,000 cells/slide. Areas evaluated for Factor VIII- and VEGF-staining varied from 1–8 mm^2. Five tumors were evaluated from each treatment group.

Data from quantitative image analysis were analyzed by the Wilcoxon Mann-Whitney test. For proliferation and apoptosis, data were expressed as the percentage of positive cells/section and calculated as the mean ± SD for each tumor. For Factor VIII and VEGF staining, data were expressed as the percent area with staining signal *versus* the total section area viewed. These data were calculated as medians ± SE for each tumor.

Table 1 *In vitro evaluation of R115777 with isolated enzymes and intact cells*

Parameter	IC_{50} (nM with 95% confidence limits) or % inhibition at highest tested concentration
Isolated FPT	
Lamin B CVIM peptide	0.86 (0.61–1.2)
K-RasB CVIM peptide	7.9 (6.8–2.37)
Isolated GGPT I	
Lamin B CVIL peptide	40% at 50 μM
Substrate-dependent growth of transfected NIH 3T3 fibroblasts	
Untransfected	0% at 500 nM
T24 H-*ras*	1.7 (1.3–2.4)
v-*raf*	97 (74–131)

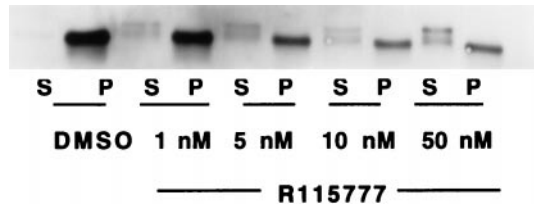

Fig. 2. R115777-inhibition of Ras ($p21^{ras}$) processing in intact NIH 3T3 cells stably transfected with the T24 H-*ras* oncogene (T24 cells). Cells grown in monolayer culture were treated with the indicated concentrations of R115777 for 3 days. Cell lysates were fractionated by centrifugation at 100,000 × *g* for 60 min into a soluble (*S*) and total particulate (*P*) fractions. Cell fractions were separated by electrophoresis on 10–20% gradient SDS polyacrylamide slab gels. Separated proteins were transferred to an Immobilon-P membrane and stained for total Ras with a pan-ras antibody. The stained Ras protein bands were detected with a horseradish peroxidase-conjugated secondary antibody and Amersham's Enhanced Chemiluminescence reagents. The bands were visualized by exposing X-ray films for 1–3 min.

RESULTS

***In Vitro* Activity.** R115777 inhibited isolated human FPT with IC_{50}s of 0.86 nM and 7.9 nM observed for a lamin B peptide and for the K-RasB peptide, respectively (Table 1). Consistent with this difference in potency for the two peptide substrates, kinetic studies revealed that R115777 was a competitive inhibitor for both the K-ras and lamin B1 peptide substrates (K_i = 0.5 nM) and noncompetitive for the farnesylpyrophosphate substrate (data not shown). PGGT I activity was virtually insensitive to R115777, with only 40% inhibition of enzyme activity observed at 50 μM R115777.

R115777 penetrated cells quite readily, as evidenced by the activity of the compound in intact cells at nanomolar concentrations. The proliferation of T24 H-*ras*-transformed NIH3T3 cells was inhibited by R115777, with an IC_{50} of 1.7 nM, whereas parental NIH 3T3 cells were unaffected by up to 500 nM R115777. The proliferation of NIH 3T3 cells transfected with an activated v-*raf* oncogene was also inhibited, but at higher concentrations (IC_{50} = 97 nM). As has been reported previously for other FTIs, the inhibition of T24 H-*ras*-transformed NIH 3T3 cell proliferation by R115777 was accompanied by a morphological reversion of the H-*ras*-transformed phenotype to a quiescent, contact-inhibited phenotype with effects observed from 0.5–50 nM (data not shown; 10, 11).

The farnesylation of Ras protein was studied in T24 H-*ras*-transformed NIH3T3 cells by Western blot analysis with a pan-Ras antibody. Cells treated with 0.5–50 nM R115777 displayed a concentration-dependent accumulation of Ras immunoreactivity in the cytosol with a concomitant reduction of processed, particulate Ras immunoreactivity (Fig. 2). Visually obvious responses were obtained within the concentration ranges that inhibited cellular proliferation. However, antiproliferative and morphological effects were observed at R115777 concentrations lower than the 10-nM concentration that was required to deplete prenylated Ras. Therefore, depletion of fully processed, activated Ras protein was not required for the cellular effects of R115777.

Summarized in Table 2 are the results from examining the substrate-dependent proliferation of 53 human tumor cell lines.[4] DNA prepared from each of the cell lines was analyzed for the presence of mutations in N-*ras* and K-*ras* at codons 12, 13, and 61 and in H-*ras* at codons 12 or 61 and position 2719 of intron D. Overall, 75% of the cell lines were sensitive to the antiproliferative effects of R115777 irrespective of *ras* gene mutations. Sensitivity was operationally defined as a 50% reduction in cell counts at concentrations of ≤100 nM.

[4] The complete set of data can be obtained from the National Auxiliary Publications Service, c/o Microfiche Publications, P.O. Box 3513, Grand Central Station, New York, NY 10163-3513. Phone: (516) 481-2300; Fax:(516) 481-6213.

Table 2 *Summary of antiproliferative effects of R115777 in 53 human tumor cell lines grouped by ras gene status*

	R115777-sensitive (IC_{50} <100 nM)	R115777-resistant
Ras gene status	Percent % (actual incidence)	Percent % (actual incidence)
Ras mutation (any *ras* gene)	65% (13/20)	35% (7/20)
ras wild type	82% (27/33)	18% (6/33)
N-*ras* or H-*ras* mutation	100% (6/6)[a]	0% (0/6)
K-*ras* mutation	50% (7/14)[b,c]	50% (7/14)

[a] N-*ras* plus H-*ras* mutants compared with *ras* wild type: sensitivity does not correlate with *ras* mutation by χ^2 test.
[b] K-*ras* mutants compared with *ras* wild type: sensitivity correlates with *ras* mutation status.
[c] K-*ras* mutants compared with N-*ras* plus H-*ras* mutants: sensitivity correlates with K-*ras* mutation status.

Table 3 *Antiproliferative effects of R115777: representative data for different tumor tissue types*

		Sensitivity to R115777	*Ras* gene status
Tumor	Cell line	IC_{50} (nM)	Gene (codon)
Pancreatic	SU86.86	9.5	K-*ras* (12)
	CAPAN-2	16	K-*ras* (12)
	PANC-1	>500	K-*ras* (12)
	AsPC-1	>500	K-*ras* (12)
	CAPAN-1	>500	K-*ras* (12)
Bladder	T24	5.2	H-*ras* (12)
	RT4	2.7	Wild type
	5637	27	Wild type
	HT-1197	1.7	H-*ras* (61)
	J82	4.6	Wild type
Melanoma	C32	6.3	Wild type
	RPMI 7951	111	Wild type
	SK-MEL-2	50	N-*ras* (61)
	SK-MEL-3	15	Wild type
	SK-MEL-5	6.8	Wild type
	SK-MEL-25	8.3	Wild type
	WM-115	3.2	Wild type
Lung	NCI-H460	>500	K-*ras* (61)
	NCI-H292	6.5	Wild type
	A549	>500	K-*ras* (12)
	NCI H441	36	K-*ras* (12)
Rhabdomyo-sarcoma	A673	3.9	Wild type
	Rd	9	N-*ras* (61)
	Hs769T	44	Wild type
	A204	4.8	Wild type

Cell lines bearing H-*ras* or N-*ras* mutations were among the most sensitive to R115777, with IC_{50}s for inhibition of proliferation <10 nM. No evidence for resistance to R115777 was observed in N-*ras* mutated cell lines, as has been suggested previously (18). However, 50% of the cell lines bearing K-*ras* mutations were resistant to R115777. Cell lines bearing K-*ras* mutations that did respond to R115777 required higher concentrations, with IC_{50}s ranging from 10–100 nM. Approximately 80% of the cell lines with wild-type *ras* were sensitive to R115777, which was consistent with previous data (14). Some clustering of sensitivity to R115777 was observed for tumor cell lines from similar tissue origins. For example, human bladder tumor, rhabdomyosarcoma, and melanoma cell lines were among the most sensitive to R115777, with cells bearing wild-type *ras* or *ras* mutations virtually indistinguishable in their responses (Table 3). Data for lung and pancreatic tumor cell lines are also summarized in Table 3 to exemplify the resistance observed in cell lines bearing K-*ras* mutations. In contrast to previous publications, A549 cells were relatively insensitive to R115777 (24, 30). This may reflect differences in experimental parameters as the former studies were conducted under conditions of anchorage-independent growth, which is an important consideration when assessing FTIs (31). Overall, the sensitivity of tumor cell lines to the FTI R115777 were consistent with data reported for cell line sensitivity to the FTI L-744,832 (14).

The CAPAN-2 cell line was selected as a human tumor cell line bearing a K-*ras* (12) mutation for additional examination of total cellular protein prenylation. Western immunoblot analysis using antibodies to lamin B and a pan-Ras antibody revealed a concentration-dependent accumulation of immunoreactivity in the soluble fraction from 1–100 nM R115777, which was interpreted as an accumulation of unfarnesylated protein (Fig. 3*A*). The majority of the pan-Ras immunoreactivity shifted to the cytosol was cross-reactive with an N-*ras* antibody (Fig. 3*B*). No H-*Ras* immunoreactivity was detected in CAPAN-2 particulate or soluble fractions. Immunoprecipitation before Western blot analysis was required to detect the low levels of K-Ras immunoreactivity in particulate fractions of CAPAN-2 cells. Although an increase in K-Ras immunostaining was noted after treatment with R115777, no increase in soluble K-Ras immunoreactivity (Fig. 3*C*) was noted. R115777 did not alter the distribution of Rap1a immunoreactivity, a geranylgeranylated protein, or RhoB immunoreactivity, a protein that can be farnesylated or geranylgeranylated (Fig. 3*A*). The results were consistent with the selectivity of R115777 observed in studies with isolated enzyme.

***In Vivo* Activity.** Data from *in vivo* tumor studies with R115777 are summarized in Table 4. A b.i.d. dosing schedule for R115777 was determined from plasma pharmacokinetics in mice (data not shown). Oral administration of R115777 at doses of 6.25, 12.5, and 25 mg/kg

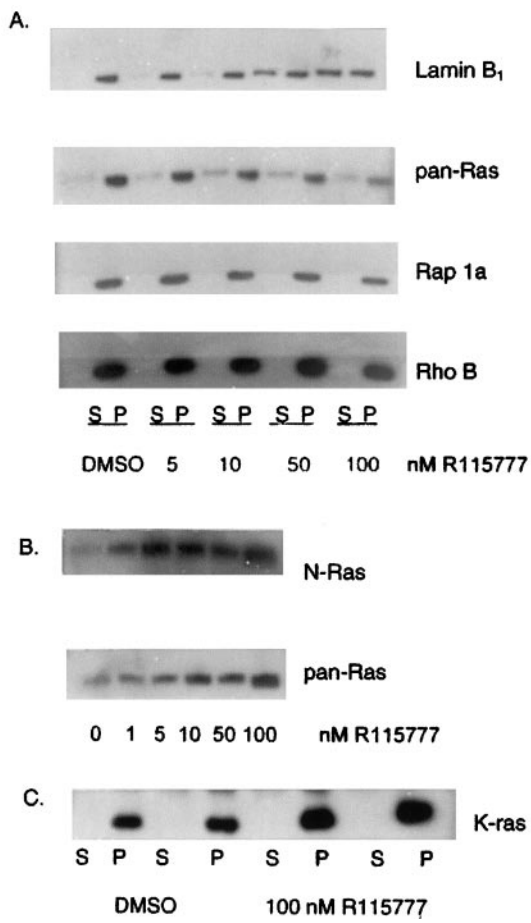

Fig. 3. Selective inhibition by R115777 of Ras protein and lamin B processing in intact CAPAN-2 human pancreatic tumor cells. Cells grown in monolayer culture were treated with the indicated concentrations of R115777 for three days and fractionated and analyzed for the indicated antigens as described in Fig. 2. *A*, distribution of lamin B1, pan-Ras, Rho B, and Rap1 immunoreactivity in soluble (*S*) and particulate (*P*) fractions after treatment with R115777. *B*, cross-reactivity of the increased soluble pan-Ras immunoreactivity induced by R115777 treatment with an antibody recognizing N-Ras. *C*, failure of treatment with 100 nM R115777 to induce the appearance of soluble K-Ras immunoreactivity detected after immunoprecipitation with Y13–259 anti-Ras antibody.

Table 4 *Antitumor effects of daily administration of R115777 in nude mouse subcutaneous tumor xenografts*

Tumor (origin)	*ras* gene status	Length of treatment (days)	R115777 dose[a] (mg/kg b.i.d)	Final tumor weight (g)[b]	% inhibition tumor growth
T24 F1 (NIH 3T3)	H-*ras* (12)	15	Vehicle	1.78 ± 0.41 (a)	
			R115777		
			6.25	0.83 ± 0.15 (a)	52%
			12.5	0.29 ± 0.07 (b)	84%
			25	0.25 ± 0.08 (b)	86%
CAPAN-2 (pancreatic)	K-*ras* (12)	18	Vehicle	1.05 ± 0.22 (a)	
			R115777		
			25	0.96 ± 0.19 (a)	8%
			50	0.42 ± 0.09 (b)	59%
			100	0.24 ± 0.06 (b)	76%
LoVo (colon)	K-*ras* (12)	32	Vehicle	0.91 ± 0.12 (a)	
			R115777		
			25	0.82 ± 0.14 (ab)	11%
			50	0.29 ± 0.07 (bc)	68%
			100	0.17 ± 0.04 (c)	81%
C32 (melanoma)	wild type	29	Vehicle	1.88 ± 0.16 (a)	
			R115777		
			25	0.99 ± 0.10 (ab)	48%
			50	0.45 ± 0.05 (bc)	76%
			100	0.18 ± 0.02 (c)	90%

[a] Administered by oral gavage twice daily in 20% β-cyclodextrin in 0.1 N HCl in a volume of 0.1 ml/10 gm body weight. Treatments began 3 days after tumor cell inoculation.
[b] Values are means ± SE for $N = 12–15$ animals/treatment group. Results of ANOVA plus Dunnett's Multiple Range tests are presented in parentheses where treatments with the same letter are not statistically significant ($P < 0.05$).

(b.i.d.) to nude mice bearing T24 tumors suppressed the growth of tumors during the 14 days of administration. Tumor growth measured as postmortem tumor weight was inhibited by 56%, 84%, and 86% at the three respective dose levels. Consistent with the *in vitro* cell proliferation data, higher doses of R115777 were required to inhibit the growth of tumors bearing K-*ras* mutations. *In vitro*, R115777 inhibited the proliferation of LoVo human colon tumor cells bearing a K-*ras* mutation with an IC_{50} of 16 nM. In nude mice bearing LoVo tumors, doses of 50 and 100 mg/kg were again required to significantly inhibit tumor growth by 68% and 81%, respectively, as determined from postmortem tumor weights after 32 days of treatment. Similar results were obtained for the CAPAN-2 tumors. The C32 melanoma was selected as a representative wild-type *ras* tumor for *in vivo* evaluation. *In vitro*, R115777 inhibited the proliferation of C32 melanoma with an IC_{50} of 6 nM (Table 3). Oral administration of R115777 at doses of 25, 50, and 100 mg/kg, b.i.d. inhibited the growth of C32 tumors by 48%, 76%, and 90% respectively. In all tumor studies, the weekly measurements of tumor area were consistent with the effects of R115777 on postmortem tumor weights (data not shown). Significant changes in body weight were not observed for R115777 treatment (data not shown). Analysis of protein prenylation was attempted in postmortem tumor samples but was not successful because of the presence of mouse antigens with apparent molecular masses of 60 kDa and 25 kDa, which crossreacted with our antimouse IgG secondary antibodies used in Western blot analysis.

Tumor Histology. The results from histological analysis of human tumor xenografts treated with R115777 are summarized in Table 5. In CAPAN-2 tumors, an antiproliferative effect was observed as statistically significant reductions of BrdUrd-labeling at doses of 50 and 100 mg/kg. A modest but significant increase in apoptosis was also observed at the 100 mg/kg dose level. By using combined Factor VIII staining with ISEL, apoptotic cells were found to be relegated to the endothelial cells of the CAPAN-2 tumor vasculature (Fig. 4). Despite this apparent antiangiogenic event, no significant changes in markers related to angiogenesis (Factor VIII or VEGF) could be detected in CAPAN-2 tumors. In contrast, a marked reduction in the endothelial cell Factor VIII-staining was observed in LoVo human colon tumors, with reductions of 45% and 60% observed at 25 and 50 mg/kg, respectively. LoVo tumors from animals treated with the 100 mg/kg dose of R115777 were too small to prepare for histology. Modest reductions in VEGF staining were also observed, but these did not achieve statistical significance. No significant changes in apoptosis or BrdUrd labeling were observed in LoVo tumors from R115777-treated mice. In the C32 melanoma tumors, yet another profile of

Table 5 *Quantitative image analysis of histological changes produced by R115777 treatment of human tumor xenografts*

		Apoptosis[a]	Proliferation[a]	Angiogenesis[b]	
Tumor (origin)	Treatment	ISEL	BrdU[c]/Ki-67[d]	Factor VIII	VEGF
Lo Vo (colon)	Vehicle	1.99 ± 0.70	30.3 ± 1.67	3.26 ± 0.41	11.6 ± 1.26
	R115777				
	25 mg/kg	3.10 ± 0.98	25.2 ± 7.68	1.76 ± 0.39[e]	8.88 ± 2.52
	50 mg/kg	2.90 ± 0.53	22.1 ± 8.10[e]	1.29 ± 0.29[e]	7.21 ± 1.54
CAPAN-2 (pancreatic)	Vehicle	5.54 ± 3.00	27.2 ± 2.37	2.16 ± 0.34	41.3 ± 3.90
	R115777				
	50 mg/kg	9.56 ± 4.26	21.9 ± 1.54[e]	2.94 ± 0.76	41.2 ± 1.80
	100 mg/kg	10.6 ± 3.00[e]	13.0 ± 0.93[e]	2.43 ± 0.81	37.2 ± 2.34
C32 (melanoma)	Vehicle	4.38 ± 2.90	30.4 ± 16.1	6.8 ± 0.42	38.1 ± 3.07
	R115777				
	25 mg/kg	21.7 ± 19.7[e]	35.1 ± 14.4	6.09 ± 0.50	39.1 ± 2.88
	50 mg/kg	44.2 ± 23.6[e]	37.7 ± 6.53	4.98 ± 0.30	36.9 ± 3.12
	100 mg/kg	42.0 ± 26.8[e]	35.2 ± 7.16	5.13 ± 0.64	43.5 ± 4.05

[a] Data expressed as the percentage of the area per slide with staining signal for VEGF or Factor III. Values are means ± SD.
[b] Data expressed as the percentage of cells staining positive.
[c] Analysis of Lo Vo and CAPAN-2 tumors only.
[d] Analysis of C32 melanoma.
[e] Statistically significant ($P < 0.05$) form vehicle controls by Wilcoxon Mann-Whitney U Test.

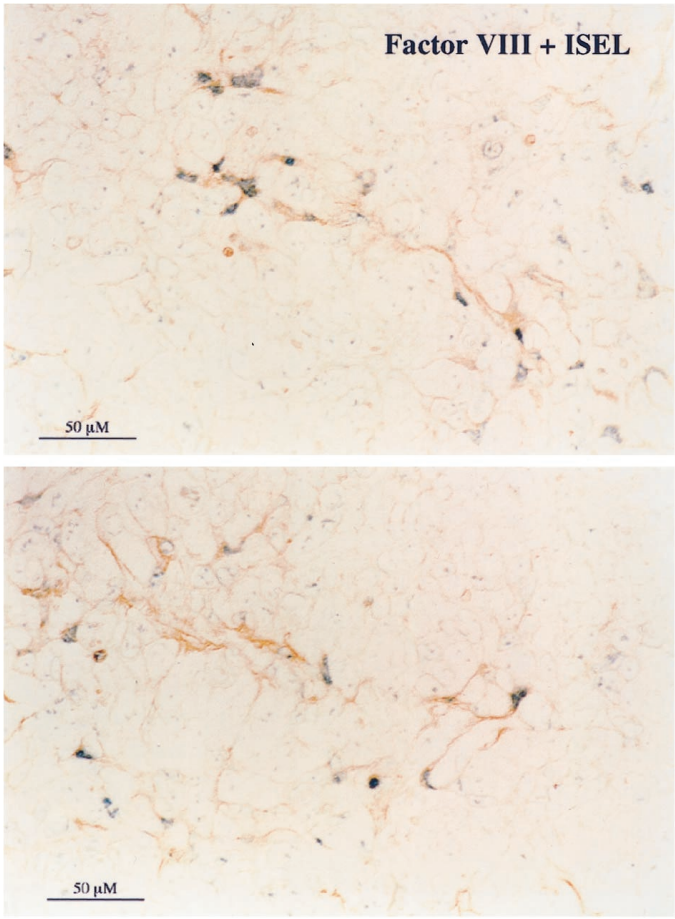

Fig. 4. Histology of CAPAN-2 human pancreatic tumors after treatment with R115777. CAPAN-2 tumor sections were subjected to combined Factor VIII immunostaining (*brown*) and ISEL labeling (*black*) to reveal that treatment with R115777 (100 mg/kg b.i.d. for 35 days) induced apoptosis in the endothelial cells of the tumor vasculature.

responses to R115777 was observed. R115777 induced a marked, dose-related increase in tumor cell apoptosis. Apoptosis increased from 4.4% in vehicle-treated controls to 22% at 25 mg/kg. At the highest tested doses of 50 and 100 mg/kg, the response appeared to reach a maximum of 41–44% incidence of apoptosis. Staining for the proliferation marker Ki67, VEGF, and Factor VIII were not affected by treatment with R115777 in the C32 melanoma tumors.

DISCUSSION

R115777 was a potent inhibitor of isolated human FPT that was competitive for the CAAX peptide substrate. The molecule was selective for FPT *versus* PGGT I despite having no obvious structural relationships to the CAAX recognition motif, which is the basis of selectivity for these two similar enzymes (31, 32). Earlier leads in the chemical series confirmed that the imidazole group is the central pharmacophore prompting the hypothesis that the imidazole interacts with the coordination structure of the zinc catalytic site (33, 34). As with other inhibitors that are competitive for the peptide-binding site, R115777 exhibited a loss of potency with a polylysine containing K-RasB peptide substrate (15).

To a degree, the loss of potency with K-RasB at the level of the enzyme was reflected in studies in intact cells *in vitro*. Cell lines with N-*ras* or H-*ras* mutations responded to lower concentrations of R115777 than did the cell lines bearing K-*ras* mutations. These findings are consistent with previously published studies, wherein tumors bearing mutant H-*ras* appear to be far more sensitive to FTIs than tumors bearing K-*ras* mutations (9, 10, 19, 20, 35, 36). Additionally, the presence of K-*ras* mutations correlated with resistance to R115777. The latter observation was consistent with resistance to FTIs being conferred by K-RasB protein geranylgeranylation via PGGT I when the farnesyl protein transferase pathway is inhibited (16–18). At the biochemical level, the involvement of K-RasB with the cellular effects of R115777 could not be substantiated. CAPAN-2 human pancreatic tumor cells responded to R115777 *in vitro* and *in vivo*. However, unprocessed K-RasB could not be detected at concentrations of R115777, which inhibited the prenylation of lamin B and N-Ras. The data suggested that the mutant K-RasB protein underwent alternative prenylation, but the postulated resistance to the FTI R115777 was absent. The findings support a role for other farnesylated targets mediating the response to the FTI R115777, as has been suggested previously (16–18, 37). Similar results were recently reported for viral-K-*ras* transgenic mice wherein the FTI L-744,832 produced antitumor effects in the K-RasB-driven tumors without effects on K-RasB prenylation (38). The activity of R115777 in Raf-transformed NIH 3T3 fibroblasts lends additional support to this concept. Despite the conflicting data, gain of geranylgeranylated RhoB remains an attractive hypothesis to explain discordance between Ras processing and the effects of FTIs (21, 22, 33). Although the Ras proteins may not be the primary farnesylated protein required for the activity of FTIs, expression of the different mutant Ras isoforms, in particular K-RasB, does appear to influence the relative sensitivity of tumor cells to this class of compound. Whether this reflects an interaction of farnesylated K-RasB signaling pathway with geranylgeranyl RhoB or the function of centromere-associated proteins is an interesting area for additional research. A point of convergence could be the high-affinity binding sites for prenylated K-RasB found in microtubules (39).

In studies of Ras-processing in the T24 H-*ras*-transfected NIH3T3 cells, the levels of Ras immunoreactivity consistently decreased. In contrast, the levels of other endogenous farnesylated proteins were noted to increase with the increase derived from the accumulation of unfarnesylated protein. This was also apparent in the immunostaining for K-Ras, which remained as a single membrane-ssociated band in CAPAN-2 cells treated with R115777. Although it has not been systematically explored, the findings suggest the possibility of a feedback to protein expression involving protein trafficking or prenylation. Consistent with the present studies, such a mechanism would not be expected to regulate expression from transfected *ras* genes, which carry engineered promoters.

In four tumor models, R115777 demonstrated significant antitumor effects when administered b.i.d. by the oral route. Although the sensitivity of the cell lines to the antiproliferative effects of R115777 *in vivo* mirrored the relative sensitivity of tumors *in vitro*, histological studies revealed that the responses elicited by R115777 in xenografts involved far more than antiproliferative effects. Computer-assisted quantitative image analysis revealed that R115777 treatment produced predominantly an antiproliferative effect in CAPAN-2 pancreatic tumors, which was accompanied by an induction of apoptosis relegated to the host endothelial cells of the tumor vasculature. A prominent antiangiogenic effect was observed in LoVo colon tumors, whereas a marked induction of apoptosis was noted in C32 melanoma tumors. The latter effect could not be observed in C32 melanoma cells cultured as monolayers *in vitro* (data not shown). The effects of R115777 in C32 melanoma are reminiscent of the report that FTI L-739,749 could produce apoptotic effects under conditions of anchorage-independent growth but not in monolayer cultures (40). Either blockade of Ras signaling via the PI3 kinase and Akt pathway or gain of geranygeranylated RhoB could account for the induction of apoptosis *in vivo* (23, 41). The emergence of additional antitumor

activities in test systems more complex than monolayer culture is consistent with FTIs acting to revert to the transformed phenotype, because transformation encompasses survival and proliferation in tumor xenografts.

In conclusion, R115777 is a p.o.-active FTI that demonstrated antitumor effects at nontoxic doses in mice. The variety of histological responses produced by treatment with R115777 suggested that modification of aspects of the malignant phenotype concerned with host-tumor interactions might be an important component of FTI effects.

REFERENCES

1. Jackson, J. H., Cochrane, C. G., Bourne, J. R., Solski, P. A., Buss, J. E., and Der, C. J. Farnesol modification of Kirsten-ras exon 4B protein is essential for transformation. Proc. Natl. Acad. Sci. USA, *87:* 3042–3026, 1990.
2. Moodie, S. A., Willumsen, B. M., Weber, M. J., and Wolfman, A. Complexes of ras-GTP with raf-1 and mitogen-activated protein kinase. Science (Washington DC), *260:* 1658–1661, 1993.
3. Egan, S. E., Giddings, B. W., Brooks, M. W., Buday, L., Sizeland, A. M., and Weinberg, R. A. Association of Sos Ras exchange protein with Grb2 is implicated in tyrosine kinase signal transduction and transformation. Nature (Lond.), *363:* 45–51, 1993.
4. Stokoe, D., Macdonald, S. G., Cadwallader, K., Symons, M., and Hancock, J. F. Activation of Raf as a result of recruitment to the plasma membrane. Science (Washington DC), *264:* 1463–1467, 1994.
5. Kato, K., Cox, A. D., Hisaka, M. M., Graham, S. M., Buss, J. E., and Der, C. J. Isoprenoid addition to Ras protein is the critical modification for its membrane association and transforming activity. Proc. Natl. Acad. Sci. USA, *89:* 6403–6407, 1992.
6. Gutierrez, J. L., Magee, A. I., Marshall, C. J., and Hancock, J. F. Post-translational processing of $p21^{ras}$ is two step and involves carboxyl-methylation and carboxyterminal proteolysis. EMBO J., *8:* 1093–1098, 1989.
7. Otto, J. C., Kim, E., Young, S. G., and Casey, P. J. Cloning and characterization of a mammalian prenyl protein-specific protease. J. Biol. Chem., *272:* 8379–8382, 1999.
8. Reiss, Y., Goldstein, J. L., Seabra, M. C., Casey, P. J., and Brown, M. S. Inhibition of purified $p21^{ras}$ farnesyl:protein transferase by Cys-AAX peptides. Cell, *62:* 81–88, 1990.
9. Gibbs, J. B. Ras C-terminal processing enzymes: new drug targets? Cell, *65:* 1–4, 1991.
10. James, G. L., Goldstein, J. L., Brown, M. S., Rawson, T. E., Somers, T. C., McDowell, R. S., Crowley, C. W. Lucas, B. K., Levinson, A. D., and Marsters, J. C., Jr. Benzodiazepine peptidomimetics: Potent inhibitors of ras farnesylation in animal cells. Science (Washington DC), *260:* 1937–1942, 1993.
11. Kohl, N. E., Mosser, S. D., deSolms, J., Giuliani, E. A., Pompliano, D. L., Graham, S. L., Smith, R. L., Scolnick, E. M., Oliff, A., and Gibbs, J. B. Selective inhibition of ras-dependent transformation by a farnesyltransferase inhibitor. Science (Washington DC), *260:* 1934–1937, 1993.
12. Lerner, E. C., Quian, Y., Blaskovich, M. A., Fossum, R. D., Vogt, A., Sun, J., Cox, A. D., Der, C. J., Hamilton, A. D., and Sebti, S. M. Ras CAAX peptidomimetic FTI-277 selectively blocks oncogenic ras signaling by inducing cytoplasmic accumulation of inactive ras-raf complexes. J. Biol. Chem., *270:* 26802–26806, 1995.
13. Cox, A. D., and Der, C. J. Farnesyltransferase inhibitors and cancer treatment: targeting simply Ras? Biochem. Biophys. Acta *1333:* F51–F71, 1997.
14. Sepp-Lorenzino, L., Ma, Z., Rands, E., Kohl, N. E., Gibbs, J. B., and Rosen, N. A peptidomimetic inhibitor of farnesyl:protein transferase blocks the anchorage-dependent and independent growth of human tumor cell lines. Cancer Res., *55:* 5302–5309, 1995.
15. James, G. L., Goldstein, J. L., and Brown, M. S. Polylysine, and CVIM sequences of *K*-rasB dictate specificity of prenylation and confer resistance to benzodiazepine peptidomimetic *in vitro*. J. Biol. Chem., *270:* 6221–6226, 1995.
16. James, G., Goldstein, J. L., and Brown, M. S. Resistance of *K*-$rasB^{v12}$ proteins to farnesyltransferase inhibitors in Rat1 cells. Proc. Natl. Acad. Sci. USA, *93:* 4454–4458, 1996.
17. Rowell, C. A., Kowalczyk, J. J., Lewis, M. D., and Garcia, A. M. Direct demonstration of geranylgeranylation and farnesylation of Ki-ras *in vivo*. J. Biol. Chem., *272:* 14093–14097, 1997.
18. Whyte, D. B., Kirschmeier, P., Hockenberry, T. N., Nunez-Olivia, I., James, L., Catino, J. J., Bishop, W. R., and Pai, J-K. *K*- and *N*-ras are geranylgeranylated in cells treated with farnesylprotein transferase inhibitors. J. Biol. Chem., *272:* 14459–14464, 1997.
19. Liu, M., Bryant, M. S., Chen, J., Lee, S., Yaremko, B., Lipari, P., Malkowski, M., Ferrari, E., Nielson, L., Prioli, N., Dell, J., Sinha, D., Syed, J., Korfmucher, W. A., Nomeir, A. A., Lin, C-C., Wang, L., Taveras, A. G., Doll, R. J., Njorge, F. G., Mallams, A. K., Remiszewski, S., Catino, J. J., Girijavallabhan, V. M., Kirschmeier, P., and Bishop, W. R. Antitumor activity of SCH 66336, an orally bioavailable tricyclic inhibitor of farnesyl protein transferase, in human tumor xenograft models and Wap-*ras* transgenic mice. Cancer Res., *58:* 4947–4956, 1998.
20. Sun, J., Qian, Y., Hamilton, A. D., and Sebti, S. M. Ras CAAX peptidomimetic FTI 276 selectively blocks tumor growth in nude mice of a human lung carcinoma with *K*-ras mutation and p53 deletion. Cancer Res., *55:* 4243–4247, 1995.
21. Lebowitz, P. F., Casey, P. J., Prendergast, G. C., and Thissen, J. A. Farnesyltransferase inhibitors alter the prenylation and growth-stimulating function of RhoB. J. Biol. Chem., *272:* 15591–15594, 1997.
22. Du, W., Liebowitz, P. F., and Prendergast, G. C. Cell growth inhibition by farnesyltransferase inhibitors is mediated by gain of geranylgeranylated RhoB. Mol. Cell. Biol., *19:* 1831–1840, 1999.
23. Liu, A-X., Du, W., Liu, J-P., Jessell, T. M., and Prendergast, G. C. RhoB alteration is necessary for the apoptotic and antineoplastic responses to farnesyltransferase inhibitors. Mol. Cell. Biol., *20:* 6105–6113, 2000.
24. Ashar, H. R., James, L., Gray, D., Black, S., Armstrong, L., Bishop, W. R., and Kirschmeier, P. Farnesyl transferase inhibitors block the farnesylation of CENP-E and CENP-F and alter the association of CENP-E with the microtubules. J. Biol. Chem., *275:* 30451–30457, 2000.
25. Chen, Z., Sun, J., Pradines, A., Favre, G., Adane, J., and Sebti, S. M. Both farnesylated and geranylgeranylated rhoB inhibit malignant transformation and suppress human tumor growth in nude mice. J. Biol. Chem., *275:* 17974–17978, 2000.
26. Reiss, Y. Seabra, M. C., Goldstein, J. L., and Brown, M. S. Purification of ras farnesyl protein transferase. Methods: A Companion to Methods in Enzymology, *1:* 241–245, 1990.
27. Todd, A. V., and Iland, H. J. Rapid screening of mutant *N-ras* alleles by analysis of PCR-induced restriction sites: allele specific restriction analysis (ASRA). Leuk. Lymphoma, *3:* 293–300, 1991.
28. Yan, N., Ricca, C., Fletcher, J., Glover, T., Seizinger, B. R., and Manne, V. Farnesyltransferase inhibitors block the neurofibromatosis type I (NF1) malignant phenotype. Cancer Res., *55:* 3569–3575, 1995.
29. Bradford, M. M. A rapid and sensitive method for the quantitation of microgram quantities of protein utilizing the principle of protein-dye binding. Anal. Biochem., *72:* 248–254, 1976.
30. Lerner, E. C., Zhang, T. T., Knowles, D., Qian, Y., Hamilton, A. D., and Sebti, S. M. Inhibition of the prenylation of K-Ras, but not H- or N-Ras is highly resistant to CAAX peptidomimetics and requires both a farnesyltransferase inhibitor and a geranylgeranyltransferase I inhibitor in human tumor cell lines. Oncogene, *15:* 1283–1288, 1997.
31. Yokoyama, K., McGeady, P., and Gelb, M. H. Mammalian protein geranylgeranyltransferase-I: substrate specificity, kinetic mechanism, metal requirements and affinity labeling. Biochemistry, *34:* 1344–1354, 1995.
32. Seabra, M., Reiss, Y., Casey, P. J., Brown, M. S., and Goldstein, J. L. Protein farnesyltransferase and geranylgeranyltransferase share a common α subunit. Cell, *66:* 429–434, 1991.
33. Huang, C-C., Casey, P., and Fierke, C. A. Evidence for a catalytic role of zinc in protein farnesyltransferase. J. Biol. Chem., *272:* 20–23, 1997.
34. Strickland, C. L., Windsor, W. T., Syto, R., Wang, L., Bond, R., Wu, Z., Schwartz, J., Le, H. V., Beese, L. S., and Weber, P. C. Crystal structure of farnesyl protein transferase complexed with CaaX peptide and farnesyl diphosphate analogue. Biochemistry, *37:* 16601–16611, 1998.
35. Nagasu, T., Yoshimatsu, K., Rowell, C., Lewis, M. D., and Garcia, M. Inhibition of human tumor xenograft growth by treatment with the farnesyl transferase inhibitor B956. Cancer Res., *55:* 5310–5314, 1995.
36. Kohl, N. E., Omer, C. A., Conner, M. W., Anthony, N. J., Davide, J. P., de Solms, S. J., Giuliani, E. A., Gomez, R. P., Graham, S. L., Hamilton, K., Handt, L. K., Hartman, G. D., Kobaln, K. S., Kral, A. M., Miller, P. J., Mosser, S. D., O'Neill, T. J., Rands, E., Schaber, M. D., Gibbs, J. B., and Oliff, A. Inhibition of farnesyltransferase induces regression of mammary and salivary carcinomas in ras transgenic mice. Nat. Med., *1:* 792–797, 1995.
37. Plattner, R., Anderson, M. J., Sato, K. Y., Fasching, C. L., Der, C. J., and Stanbridge, E. J. Loss of oncogenic *ras* expression does not correlate with loss of tumorigenicity in human cells. Proc. Natl. Acad. Sci., USA, *93:* 6665–6670, 1996.
38. Omer, C. A., Chen, Z., Diehl, R. E., Conner, M. W., Chen, H. Y., Trumbauer, M. E., Gopal-Truter, S., Seeburger, G., Bhimnathwala, H., Abrams, M. T., Dvide, J. P., Ellis, M. S., Gibbs, J. B., Greenberg, I., Hamilton, K., Koblan, K. S., Kral, A. M., Liu, D., Lobell, R. B., Miller, P. J., Mosser, S. D., O'Neill, T. J., Rands, E., Schaber, M. D., Senderak, E. T., Oliff, A., and Kohl, N. E. Mouse mammary tumor virus Ki-*ras*B transgenic mic develop mammary carcinomas that can be growth-inhibited by a farnesyl:protein transferase inhibitor. Cancer Res., *60:* 2680–2688, 2000.
39. Thissen, J. A., Gross, J. M., Subramanian, K., Meyer, T., and Casey, P. J. Prenylation-dependent association of Ki-Ras with microtubules. Evidence for a role in subcellular trafficking. J. Biol. Chem., *272:* 30362–30370, 1997.
40. Lebowitz, P. F., Sakamuro, D., and Prendergast, G. C. Farnesyl transferase inhibitors induce apoptosis of Ras-transformed cells denied substratum attachment. Cancer Res., *57:* 708–713, 1997.
41. Jiang, K., Coppola, D., Crespo, N. C., Nicosia, S. V., Hamilton, A. D., Sebti, S. M., and Cheng, J. Q. The phosphoinositide 3-OH-kinase/AKT2 pathway as a critical target for farnesyltransferase inhibitor-induced apoptosis. Mol. Cell. Biol., *20:* 139–148, 2000.

Characterization of the Antitumor Effects of the Selective Farnesyl Protein Transferase Inhibitor R115777 *in Vivo* and *in Vitro*

David W. End, Gerda Smets, Alison V. Todd, et al.

Cancer Res 2001;61:131-137.